Applied Surface Science 282 (2013) 133–137

Contents lists available at SciVerse ScienceDirect

Applied Surface Science

journal homepage: www.elsevier.com/locate/apsusc

Confined laser ablation for single-shot nanoparticle deposition of silver

T. Donnelly*, J.G. Lunney

School of Physics, Trinity College Dublin, Dublin 2, Ireland

ARTICLE INFO

Article history:
Received 16 January 2012
Received in revised form 7 May 2013
Accepted 16 May 2013
Available online 29 June 2013

Keywords:
Confined laser ablation
Nanoparticle deposition
Plasma spectroscopy
Surface plasmon resonance
Pulsed laser deposition

ABSTRACT

Spatially confined laser ablation of silver was used to form long-lived dense plasma for single-shot deposition of a nanoparticle film. The expansion of the ablation plume was restricted by placing a glass substrate at 50 μm from the silver target surface. Time-resolved optical emission spectroscopy showed that the confined plasma is sustained for longer time than for free ablation. A single laser shot is sufficient to produce a layer of silver nanoparticles on the substrate. In absorption the nanoparticle layer displays a surface plasmon resonance which is comparable to films made by conventional pulsed laser deposition in vacuum.

1. Introduction

Laser ablation is the controlled removal of material from the surface of a solid target by pulsed laser irradiation. In nanosecond laser ablation a thin surface layer is heated to temperatures in the region of the boiling point and intense evaporation ensues during the laser pulse. The vapour is further heated by the laser so that by the end of the laser pulse the ablated material exists as a thin layer of dense plasma on the surface of the target. The steep pressure gradients in this plasma drive a forward-peaked expansion which produces the characteristic semi-ellipsoidal ablation plume. Laser ablation has found application in several areas, including micro-machining of solid materials, laser induced breakdown spectroscopy for elemental analysis and in pulsed laser deposition (PLD) of novel materials for research [1,2].

For PLD the laser fluence is normally chosen to be somewhat above the threshold fluence for ablation, typically ~0.3–3 J cm^{-2}. In this case the ablation depth is typically ~3–30 nm and at the end of the laser pulse the dense plasma layer on the target is ~30–100 μm thick and has a temperature of a few eV and a particle density of ~10^{18}–10^{19} cm^{-3} [3]. In vacuum, the ablated material expands freely away from the target to reach supersonic velocities, where most of the initial thermal energy is converted to the kinetic energy of the atoms and ions [4]. In conventional PLD the ablated material is condensed on a substrate placed at 3–10 cm from the target. For nanosecond PLD in vacuum of some metals, on non-wetting substrates, it has been observed that when the equivalent thickness of the metal is less than ~5 nm the film is comprised of nanoparticles (NPs) [5]. In this case NP formation occurs by surface diffusion and aggregation [6]. A background gas may be used to confine and slow down the ablation plume to allow sufficient time for nucleation of nanoparticles, which can be collected on a substrate or otherwise [7]. Femtosecond laser ablation may also be used for NP PLD, though in this case the NPs are formed by fragmentation and spinodal decomposition of the target materials arising from the very rapid heating [8]. Nanosecond pulsed laser annealing of pre-deposited thin metal films has also been shown to produce metal nanoparticle films, where the degree of nanostructuring depends on the irradiation conditions and the number of laser pulses [9].

In this paper we report on a new variation of the PLD technique whereby a flat bulk target is irradiated through a transparent substrate that is placed close to the target such that the ablated material is very strongly confined and a single laser shot is sufficient to produce measurable NP films. The ablation configuration used here is similar to that used by Heading et al. [10] to form spatially uniform high-density plasma at low temperature. Our technique bears some resemblance to laser induced forward transfer (LIFT) [11]. LIFT using a femtosecond laser has been used to fabricate 300 nm Cr droplets [12]. Our technique is distinguished form LIFT in that it is not necessary to prepare a thin film of the materials to be transferred. Our technique also has some similarity to laser ablation direct writing of metal nanoparticles where laser ablation of a metal film in a gas at atmospheric pressure confines the ablation

* Corresponding author. Tel.: +353 1 8962157.
E-mail address: tdonnell@tcd.ie (T. Donnelly).

0169-4332/$ – see front matter © 2013 Elsevier B.V. All rights reserved.
http://dx.doi.org/10.1016/j.apsusc.2013.05.083

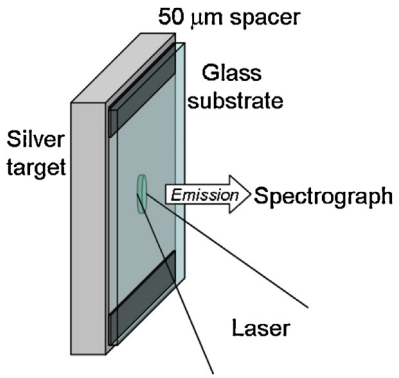

Fig. 1. Schematic diagram of the experimental setup used for confined PLD.

plume leading to back-deposition of nanoparticles on the supporting substrate [13].

2. Experimental setup

The confined PLD setup is shown in Fig. 1 where a silver target was irradiated in vacuum at 10^{-5} mbar with a 10 ns, 1064 nm laser pulse. The focused laser spot was elliptical with minor and major radii of 1.25 mm and 1.75 mm respectively and the fluence used was in the range 0.5–1.5 J cm^{-2}. A 2 mm thick soda lime glass slide was placed 50 μm above the silver target surface to spatially confine the ablation plasma. Strips of thin metal foil of 50-μm thickness were used as spacers to separate the target and the glass substrate. The deposition setup was placed on a linear motion feedthrough and moved after each shot. There was sufficient distance between ablation sites to ensure that the deposition from one shot did not influence the next. Time resolved emission spectroscopy, using a 0.25 m Czerny Turner spectrograph fitted with a gateable intensified CCD, was used to study the plasma dynamics in both confined and free ablation configurations. The spectral resolution was ~1 nm and the gate time was 10 ns. The angle of incidence of the laser beam was 45°, while the emission spectra were recorded along the target normal. The plasma density and temperature were calculated from the emission spectra using Stark width analysis and the Boltzmann plot method. The atomic data required for this analysis was taken from the PrismSPECT software database [16]. The NP films deposited on the substrate were characterized using scanning electron microscopy (SEM) and UV/visible absorption spectrometry.

3. Results and discussion

Figure 2 shows a comparison of the temporal development, in the period 0–100 ns, of the spectral emissions in the region 320–850 nm for free and confined ablation. For both cases

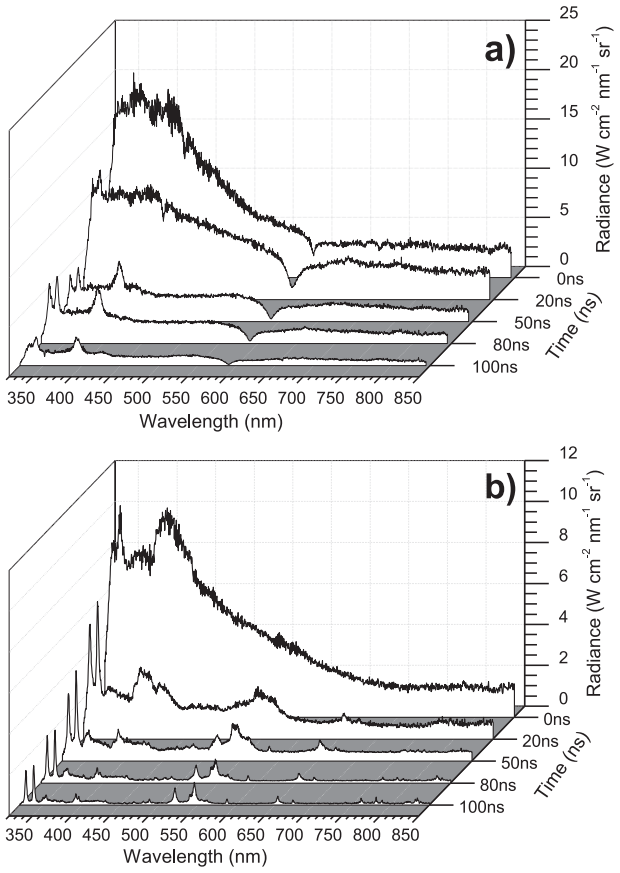

Fig. 2. Temporal variation, in the range 0–100 ns, of spectral radiance of plasma emission for: (a) confined ablation and (b) free ablation.

continuum emission is observed during the laser pulse (zero time delay), which seems to be due a combination of bremsstrahlung, radiative recombination and Stark broadened bound-bound transitions in the plasma [14,15]. For the confined case an absorption feature is observed at 590 nm which is thought to be due to resonance absorption in atomic sodium evolved from the glass through heating by UV emission form the plasma. For times up to 100 ns the emission profile in the confined geometry remains smooth while the intensity of the continuum is reduced for increasing time. In the freely expanding plasma case however, the spectral lines begin to emerge from the continuum from 50 ns onwards while the background continuum level also decreases with increasing time. At later times the intensity of the continuum reduces further and distinct line emission is observed from 100 ns after the laser pulse for the free case and 300 ns for the confined case. The prominent Ag I lines in this region are summarized in Table 1 and

Table 1
Main Ag I transitions observed in the emission spectra together with the associated atomic parameters used in the measurement of electron temperature.

Wavelength, λ (nm)	Transitions	Statistical weight		Transition probability, A_{ul} (s^{-1})	Energy of upper level, E_u (eV)
		g_u	g_l		
328.1	$5p^2P_{3/2}$–$5s^2S_{1/2}$	4	2	1.47×10^8	3.78
338.3	$5p^2P_{1/2}$–$5s^2S_{1/2}$	2	2	1.35×10^8	3.66
405.6	$6d^2D_{3/2}$–$5p^2P_{1/2}$	4	2	2.3×10^7	6.72
421.1	$6d^2D_{5/2}$–$5p^2P_{3/2}$	6	4	2.6×10^7	6.72
421.3	$6d^2D_{3/2}$–$5p^2P_{3/2}$	4	4	4.35×10^6	6.72
447.6	$7s^2S_{1/2}$–$5p^2P_{1/2}$	2	2	5.25×10^6	6.43
466.8	$7s^2S_{1/2}$–$5p^2P_{3/2}$	2	4	9.53×10^6	6.43
520.9	$5d^2D_{3/2}$–$5p^2P_{1/2}$	4	2	7.5×10^7	6.04
546.5	$5d^2D_{5/2}$–$5p^2P_{3/2}$	6	4	8.6×10^7	6.05
547.2	$5d^2D_{3/2}$–$5p^2P_{3/2}$	4	4	1.3×10^7	6.05